fractal and fractional

Article

Multifractal Features and Dynamical Thresholds of Temperature Extremes in Bangladesh

Anxin Liu [1], Zhihua Zhang [1,2,*], M. James C. Crabbe [3,4] and Lipon Chandra Das [1,5]

1 School of Mathematics, Shandong University, Jinan 250100, China; 202111946@mail.sdu.edu.cn (A.L.); liponbgc@gmail.com (L.C.D.)
2 MOE Key Laboratory of Environmental Change and Natural Disaster, Beijing Normal University, Beijing 100875, China
3 Wolfson College, Oxford University, Oxford OX2 6UD, UK; james.crabbe@wolfson.ox.ac.uk
4 Institute of Biomedical and Environmental Science & Technology, University of Bedfordshire, Luton LU1 3JU, UK
5 Department of Mathematics, University of Chittagong, Chittagong 4331, Bangladesh
* Correspondence: zhangzhihua@sdu.edu.cn

Abstract: Multifractal detrended fluctuation analysis (DFA) can extract multi-scaling behavior and measure long-range correlations in climatic time series. In this study, with the help of multifractal DFA, we investigated the scaling behavior of daily minimum/maximum temperatures during the years 1989–2019 from 34 meteorological stations in Bangladesh. We revealed spatial patterns, topographic impacts and global warming impacts of long-range correlations embedded in small and large fluctuations in temperature time series. Meanwhile, we developed a multifractal DFA-based algorithm to dynamically determine thresholds to discriminate extreme and non-extreme events in climate systems and applied it to analyze the frequency and trends of temperature extremes in Bangladesh. Compared with widely-used percentile thresholds, the extreme climate events captured in our algorithm are more reliable since they are determined dynamically by the climate system itself.

Keywords: scaling behavior; small and large fluctuations; thresholds of climate extremes; multifractal detrended fluctuation analysis

Citation: Liu, A.; Zhang, Z.; Crabbe, M.J.C.; Das, L.C. Multifractal Features and Dynamical Thresholds of Temperature Extremes in Bangladesh. *Fractal Fract.* **2023**, *7*, 540. https://doi.org/10.3390/fractalfract7070540

Academic Editor: Viorel-Puiu Paun

Received: 8 June 2023
Revised: 9 July 2023
Accepted: 9 July 2023
Published: 13 July 2023

1. Introduction

Climate change and its environmental, economic, and social consequences are widely recognized as a major set of interconnected problems facing human societies. Its impacts and costs will be large, serious, and unevenly spread globally for decades. In the 21st century, global climate change and its impacts will be more widespread, rapid, and intensifying than many people expected. The latest IPCC AR6 report indicated that without significant carbon emissions reduction over the next twenty years, the global mean temperature would be expected to reach or exceed 1.1 °C of warming since the industrial revolution [1]. Faster warming leading to extreme climate events further strengthening in terms of frequency, intensity, impact range, and duration will cause serious damage to both the natural ecosystem and the socioeconomic system.

Due to significant self-memory features in climate evolution [2], various observed climate data, arising from climate change and related fields, provide a huge amount of interconnected multifractal information. Detrended fluctuation analysis (DFA) can systematically eliminate local trend components of different orders of nonstationary climatic time series so as to detect scaling structure, self-similarity, and long-range correlation. Compared with traditional methods (e.g., autocorrelation, spectral analysis, and Hurst analysis), the advantage of the DFA method is to distinguish the inherent trends and long-range fluctuations in nonstationary climatic time series [3,4]. Currently, DFA is becoming a mainstream tool in climatic time analysis: Kurnaz (2004) found that DFA of daily maximum temperatures could distinguish different climate types [5]. Orun and Kocak (2009) used DFA to investigate daily temperatures at 52 meteorological stations in Turkey and found that all of the scaling exponents were larger than 0.5, indicating that these temperature data had long-range correlations [6]. Pierini and Telesca (2010) used DFA to investigate the 1860–2006 monthly rainfall time series recorded in five weather stations in the middle of Argentina [7]. They found that the associated DFA scaling exponents ranged between 0.54 and 0.58, and the weak persistence of the inner dynamics of rainfall meant that the dynamics of rainfall in middle Argentina were mainly driven by external factors. As a complex system always displays multi-scaling structures and DFA can only estimate a single scaling exponent statistically, multifractal DFA was proposed to reveal multifractal/multi-scaling characteristics. Kalamaras et al. (2017) used multifractal DFA to investigate the daily temperature time series from one single weather station in Greece and found that it exhibited a multifractal structure and was insensitive to local fluctuations with large magnitudes [8]. Gómez-Gómez et al. (2021) used MF-DFA to analyze daily maximum, minimum, and mean temperatures from ten weather stations in Spain and found that all these temperature variables had multifractal natures and that coastal regions had higher complexity of minimum and mean temperatures than the mainland regions [9].

In this study, with the help of multifractal DFA, we investigated the scaling behavior of daily minimum/maximum temperature data from 1989–2019 from 34 meteorological stations in Bangladesh. We revealed spatial patterns, topographic distance from the coast, global warming impacts of scaling behavior, and long-range correlations embedded in small and large fluctuations in temperature time series in Bangladesh. Moreover, we developed a multifractal DFA-based method to dynamically determine thresholds to discriminate extreme and non-extreme temperature events and used it to analyze the frequency and trends of temperature extremes in Bangladesh. Compared with widely-used percentile thresholds [10,11], extreme climate events captured in our method are more reliable since they are determined dynamically by the climate system and delete local trend impacts.

2. Study Area and Data

Bangladesh is located in South Asia, bordering India and Myanmar, with an area of about 147,500 square kilometers. As Bangladesh is located on the delta plain at the lower reaches of the Ganges, Jamuna, and Meghna rivers in the northeast of the South Asian subcontinent, its terrain is flat, and its river network is dense, leading to low ability to cope with climate disasters. Bangladesh has been rated as the most vulnerable country in the world by the IPCC. The increasing severity and frequency of extreme climate events have caused serious losses to the socioeconomic development of Bangladesh [12,13]. Agriculture is the backbone of Bangladesh's economy and always faces large-scale heavy rainfalls, high temperatures, and hurricanes [12,14,15]. The destruction of the agricultural sector by extreme weather events will directly affect the production and life of the people of Bangladesh. Bangladesh has 34 meteorological stations in Bangladesh (Figure 1). The daily observation of maximum and minimum temperatures observed at these meteorological stations from 1989 to 2019 was collected from the Bangladesh Meteorological Department (BMD) in Dhaka.

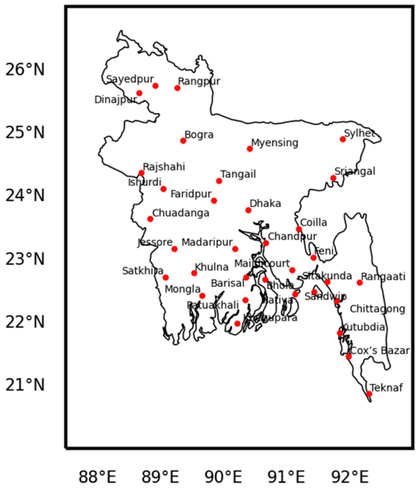

Station	Latitude	Longitude	Elevation	Zone	Station	Latitude	Longitude	Elevation	Zone
Dhaka	23.7	90.4	14	Plain	Feni	23.0	91.4	7	Plain
Sylhet	24.9	91.8	25	Mountain	Patuakhali	23.4	90.3	8	Plain
Mymensingh	24.7	90.4	16	Plain	Chuadanga	23.6	88.9	11	Plain
Faridpur	23.6	89.6	8	Plain	Mungla	22.6	89.5	4	Plain
Khulna	22.9	89.6	6	Plain	Chandpur	23.2	90.7	8	Plain
Chittagong	22.3	91.8	24	Coastal	Sandwip	22.5	91.4	6	Coastal
Cox's Bazar	21.4	92.0	6	Coastal	Bhola	22.6	91.4	4	Coastal
Jessore	23.2	89.2	12	Plain	Teknaf	20.8	92.2	6	Coastal
Satkhira	22.7	89.1	5	Plain	Sydpur	24.9	88.9	25	Mountain
Barisal	22.7	93.4	8	Plain	Srimangal	25.6	88.7	22	Mountain
Bogra	24.8	89.4	23	Mountain	Madaripur	23.2	90.2	8	Plain
Rangpur	25.8	89.3	29	Mountain	Kutubdia	22.4	92.5	4	Coastal
Dinajpur	26.1	89.1	34	Mountain	Rangamati	22.6	92.2	49	Mountain
Rajshahi	24.4	88.6	19	Mountain	MaijdeeCourt	22.8	91.1	8	Plain
Tangail	24.3	89.9	10	Plain	Hatiya	22.5	90.2	6	Coastal
Ishurdi	24.1	89.1	16	Plain	Sitakunda	23.1	91.6	10	Plain
Comilla	23.5	91.2	5	Plain	Khepupara	22.6	90.4	1	Coastal

Figure 1. Location of 34 meteorological stations in Bangladesh.

3. Multifractal Detrended Fluctuation Analysis

The detrended fluctuation analysis (DFA) retrieves intrinsic self-similarity and detects scaling and long-range correlation characteristics of fluctuations in the presence of possible trends without knowing their origin and shape [16]. Since the classic DFA can only deal with monofractal time series, its multifractal extension (multifractal DFA) was invented to determine more than one scaling exponent (multifractal) embedded in the time series [17]. The algorithm of multifractal DFA is as follows:

For a time series $\{x_k\}$ with length N, its cumulative deviation is

$$y(i) = \sum_{k=1}^{i} (x_k - \overline{x}), \quad i = 1, 2, \ldots, N$$

where $\overline{x}$ is the mean value of $\{x_k\}$. We divided the cumulative deviation sequence $\{y(i)\}$ into non-overlapping segments of size s, that is $N_s = \left(\frac{N}{s}\right)$. Since the sequence length N is not always an integer multiple of the time scale s, a small amount of data information at the end of the time series cannot be fully utilized. Therefore, the same segmentation procedure is repeated starting from the opposite end so that $2N_s$ segments can be obtained. In each segment, the data is locally detrended by a linear, quadratic, cubic, or higher-order polynomial regression $y_v(i)$. Then the mean squared residual for each segment is

$$F^2(v, s) = \frac{1}{s} \sum_{i=1}^{s} \{y[(v-1)s + i] - y_v(i)\}^2,\ v = 1, 2, \cdots, N_s$$

$$F^2(v, s) = \frac{1}{s} \sum_{i=1}^{s} \{y[N - (v - N_s)s + i] - y_v(i)\}^2,\ v = N_s + 1, N_s + 2, \cdots, 2N_s.$$

After that, the mean squared residual of all segments is accumulated and averaged:

$$F_q(s) = \left\{ \frac{1}{2N_s} \sum_{v=1}^{2N_s} \left[F^2(v, s) \right]^{\frac{q}{2}} \right\}^{\frac{1}{q}}$$

where q is often called the moment parameter. The fluctuation function $F_q(s)$ can be used to examine self-similarity structures as it performs a fluctuation measure at different segment sizes. Typically, $F_q(s)$ will increase with the segment size s. If $F_q(s)$ and s are in a power-law correlation, i.e.,

$$F_q(s) \propto s^{h(q)}$$

it means that the fluctuations in small segments are related to the fluctuations in large segments in a power-law fashion. The scaling exponent $h(q)$ may be estimated statistically through the log-long plots of $F_q(s)$ vs. s for each given q. The scaling exponent index $h(q)$ is often called a generalized Hurst index. If $h(q)$ is dependent on q, then the time series $\{x_k\}$ shows changes in multifractal nature, especially when $h(q) < 0.5$ and $\{x_k\}$ is anti-correlated; when $h(q) = 0.5$, $\{x_k\}$ is white noise; and when $h(q) > 0.5$, $\{x_k\}$ is long-range correlated [18]. When $q = 2$, the multifractal DFA is reduced to the regular DFA, and the associated $h(2)$ is just the Hurst index [3].

In this study, we used multifractal DFA to analyze daily temperatures in Bangladesh and then revealed multifractal features of its climate evolution. By comparing the difference in the fluctuation functions $F_q(s)$ of daily temperature extremes of 34 meteorological stations generated by linear, quadratic, and cubic polynomial regressions, we found that the impacts of the order of polynomial regressions on the generalized Hurst index are very slight. Figure 2 demonstrates an example of fluctuation functions $F_q(s)$ ($q = -2$, 2) of daily temperature extremes at the Dinajpur meteorological station of Bangladesh, where the segment size s ranges from 2^3 to 2^{10}. It is clear that the three fluctuation function curves are almost parallel to each other, indicating that the calculated generalized Hurst indices are almost the same. In this study, we chose quadratic polynomial regression and mainly focused on spatial patterns of generalized Hurst index distribution in Bangladesh.

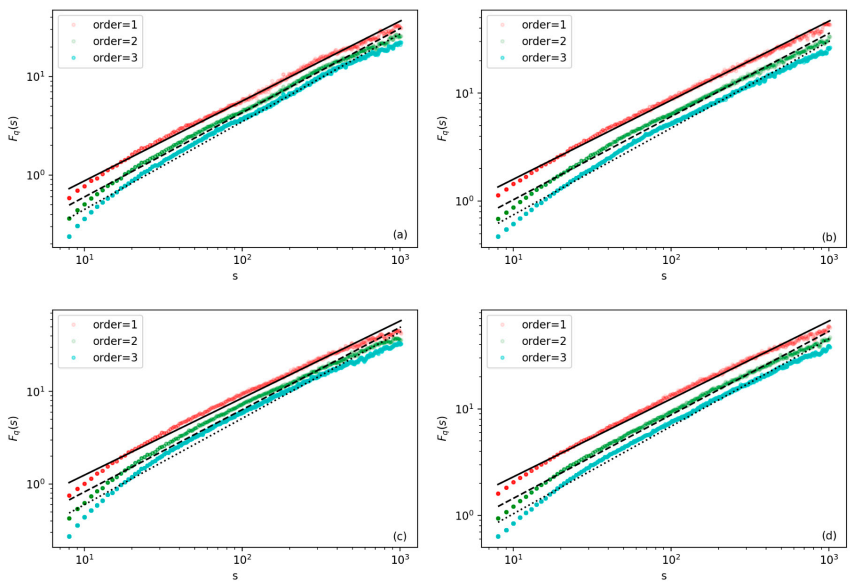

Figure 2. Fluctuation functions after detrending by first/second/third-order regression polynomials for daily minimum temperatures with (**a**) $q = -2$, (**b**) $q = 2$; and for daily maximum temperatures at Dinajpur with (**c**) $q = -2$, (**d**) $q = 2$.

4. Multifractal Features of Daily Temperatures in Bangladesh

In this section, we revealed multifractal structures of climate evolution in Bangladesh during 1989–2019 and analyzed global warming impacts on Bangladesh. In order to avoid the effects of seasonal cycles, we deseasonalized the daily minimum/maximum temperature time series from 34 meteorological stations in Bangladesh first.

4.1. Daily Minimum Temperatures

We calculated generalized Hurst indices $h(q)$ of daily minimum temperatures at all meteorological stations in Bangladesh. Figure 3 demonstrates generalized Hurst indices $h(q)$ at eight stations: Dinajpur, Barisal, Cox's Bazar, Bhola, Bogra, Chandpur, Chittagong, and Chuadanga. If the value of $h(q)$ is independent of q, it implies that the climatic time series exhibits a monofractal feature; otherwise, it exhibits a multifractal feature. From Figure 3, it is clear that the daily minimum temperatures at all stations in Bangladesh exhibited multifractal features and that generalized Hurst indices $h(q)$ decayed quickly for $q < 0$ and slowly for $q > 0$.

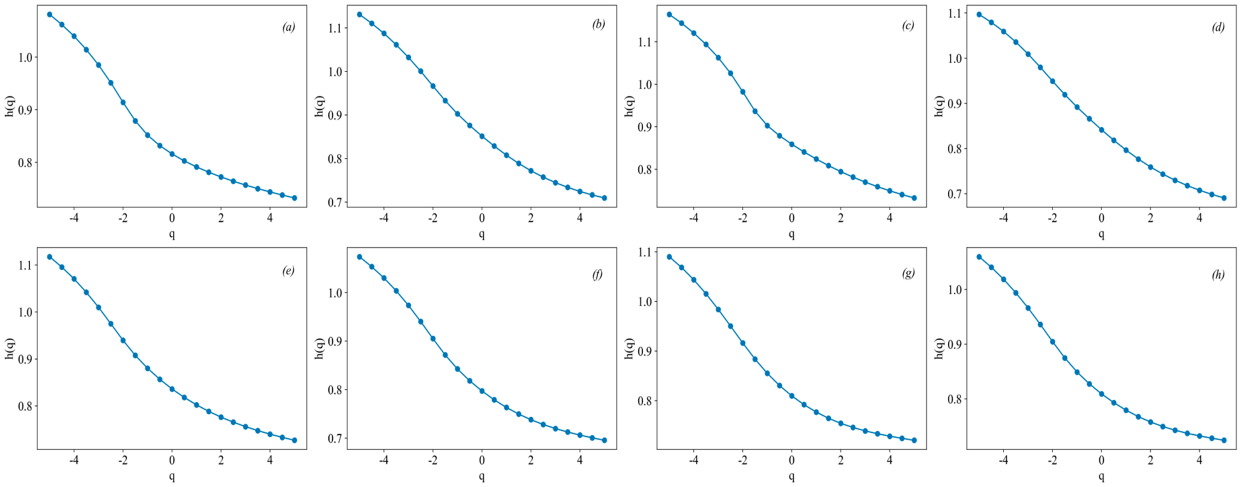

Figure 3. Generalized Hurst indices $h(q)$ of daily minimum temperatures at eight meteorological stations: (**a**) Dinajpur, (**b**) Barisal, (**c**) Cox's Bazar, (**d**) Bhola, (**e**) Bogra, (**f**) Chandpur, (**g**) Chittagong, and (**h**) Chuadanga.

We applied the multifractal DFA to the deseasonalized daily minimum temperature data in Bangladesh during 1989–2019 and then obtained the distribution of generalized Hurst indices $h(q)$ for different values of q in the whole of Bangladesh (Figure 4); Figure 4d,h demonstrate the distribution of mean generalized Hurst indices for $q \in [-3, -1]$ and $q \in [1, 3]$ with step 0.1, respectively. All generalized Hurst indices $h(q)$ are larger than 0.7, indicating the presence of a strong persistent long-range positive correlation over the whole of Bangladesh, i.e., it means that a relatively large value in the daily minimum temperature time series is most likely to be followed by other large values. Such strong persistence of the inner dynamics of daily minimum temperatures implies that historical climatic oscillation modes in each meteorological station have a larger probability of reappearing in the future, resulting in the future evolution of extremely low temperatures at each meteorological station being determined largely by local historical climate change, i.e., the dynamics of extremely low temperatures are driven mainly by internal factors.

The generalized Hurst indices of daily minimum temperatures in Bangladesh reached the maximum in southeast Bangladesh, demonstrating the strongest long-range positive correlation during 1989–2019. Southeast Bangladesh is known as the Chittagong hill tracts, which are much higher than the rest of Bangladesh (i.e., alluvial plain). High elevation differences reduced the impacts of external factors on climate in Chittagong hill tracts and then resulted in strong long-range correlations embedded in the daily minimum temperature time series. The generalized Hurst indices reached minima in the northern border and coastal areas of Bangladesh. The minimum temperature fluctuations in Bangladesh were mainly caused by the influence of atmospheric circulation in South Asia and topographic differences between land and sea. The Himalayas and the Qinghai-Tibet Plateau block the cold airflow in the central hinterland of the Eurasian continent, resulting in more impacts on minimum temperature fluctuations in the northern border than the rest of Bangladesh. Since the southern coastal regions of Bangladesh are adjacent to the Bay of Bengal, minimum temperature fluctuations in coastal regions are suppressed by the heat capacity of the oceans. Therefore, the smallest generalized Hurst indices appeared in the northern border and coastal areas of Bangladesh.

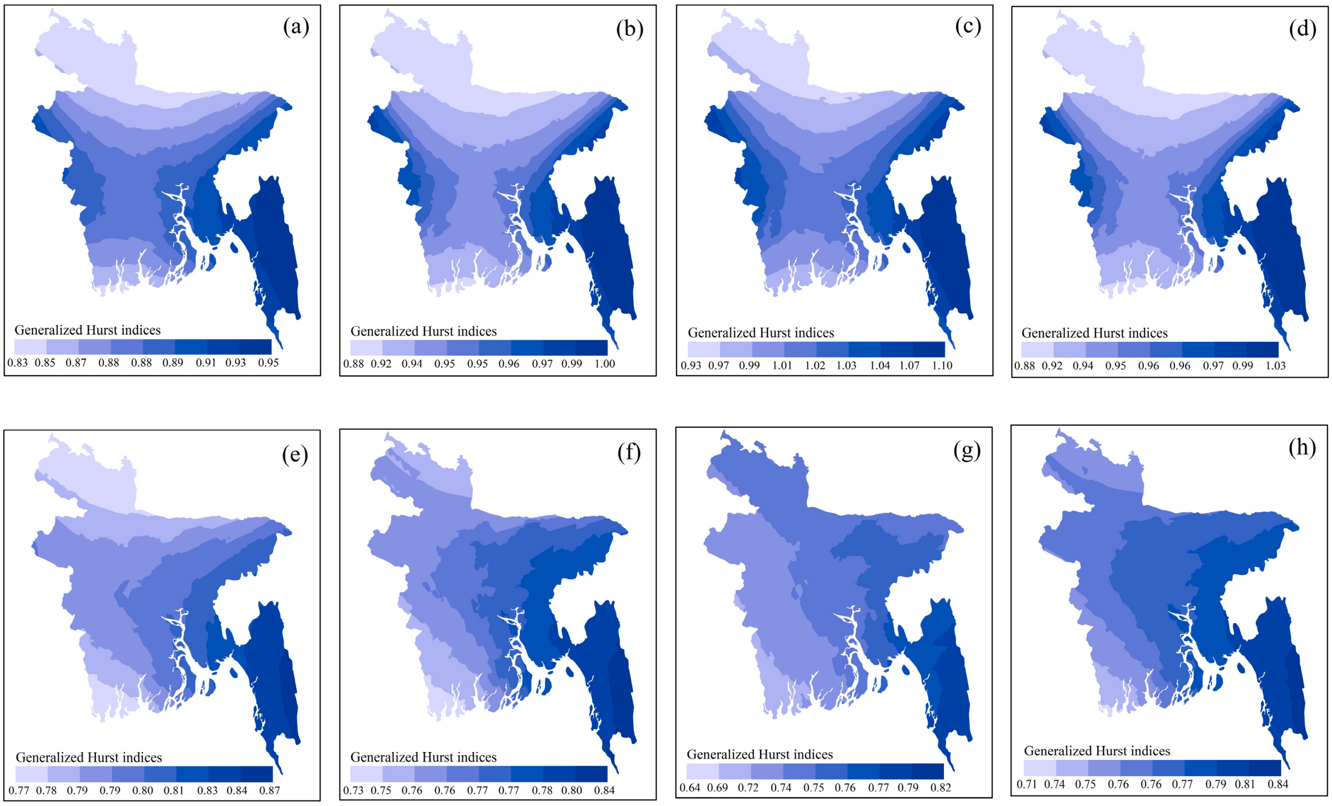

Figure 4. Distribution of (mean) generalized Hurst indices of daily minimum temperatures for different moment parameters: (**a**) $q = -1$, (**b**) $q = -2$, (**c**) $q = -3$, (**d**) $q \in [-3, -1]$, (**e**) $q = 1$, (**f**) $q = 2$, (**g**) $q = 3$, (**h**) $q \in [1, 3]$.

The scaling behavior of the daily minimum temperature in Bangladesh during 1989–2019 demonstrated two different spatial patterns (Figure 4), i.e., the distribution patterns of $h(q)$ for different negative (or positive) values of q were almost the same, But the distribution patterns of $h(q)$ for negative values of q were very different from these for positives values of q. Since segments with large fluctuations and small fluctuations in time series determine the values of $F_q(s)$ $(q > 0)$ and $F_q(s)$ $(q < 0)$ in multifractal DFA, respectively, these two spatial patterns are associated with the scaling behavior of small and large fluctuations embedded in the daily minimum temperature, respectively.

Figure 5 shows the relationship between different topographic factors and generalized Hurst indices in Bangladesh. By statistical hypothesis testing of linear regression, longitude, latitude, elevation, and distance from the coast have statistically significant impacts with a significance level (p-value) much less than 0.05 (Figure 5). During 1989–2019, longitude was positively linearly correlated with generalized Hurst indices in Bangladesh. Both latitude and distance from the coast were negatively linearly correlated. This is linked with the fact that whatever the location of the meteorological station, the distance from the coast increased roughly as the latitude decreased. Elevation seemingly has impacts on generalized Hurst indices; unfortunately, the flat terrain in the whole of Bangladesh prevents an unambiguous conclusion. The scaling behavior of both small and large fluctuations in the daily minimum temperature was revealed by generalized Hurst indices with moment parameters $q < 0$ and $q > 0$, respectively. In terms of R^2, latitude and distance from the coast had greater impacts on the scaling behavior of small fluctuations, while longitude had greater impacts on that of large fluctuations.

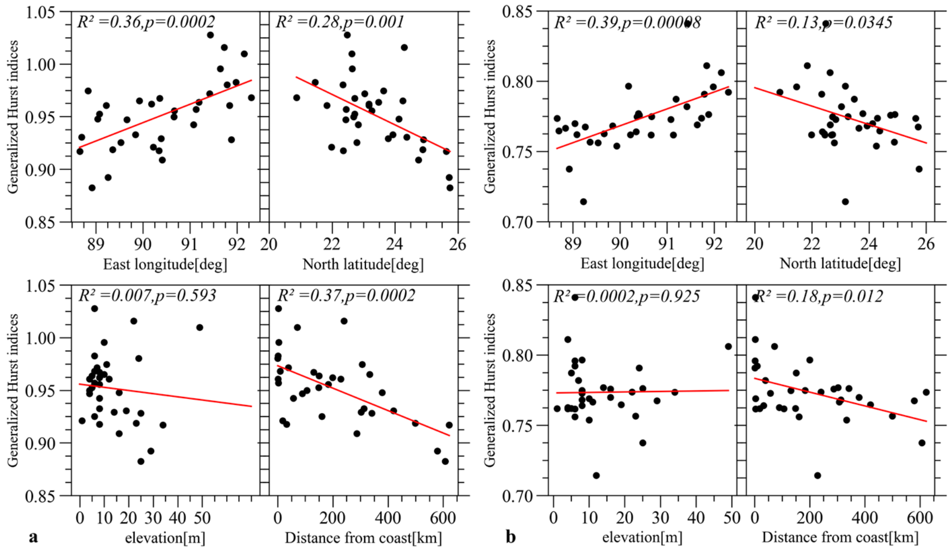

Figure 5. Scatter plots for different topographic factors and mean generalized Hurst indices of daily minimum temperature with (**a**) $q < 0$ and (**b**) $q > 0$.

Finally, we investigated the impacts of global warming on long-range correlations of daily minimum temperatures in Bangladesh (Figure 6). In order to achieve this, we divided the whole period [1989–2019] into two periods: [1989–2004] and [2005–2019]. By statistical hypothesis testing of linear regression, the difference in generalized Hurst indices during the two time periods passed a statistical significance test, and the related significance levels (p values) were 7.7505×10^{-7} ($q = -3$), 1.6932×10^{-5} ($q = -2$), 0.072598 ($q = -1$), 0.037662 ($q = 1$), 0.019166 ($q = 2$), and 0.004338 ($q = 3$). In the case of the moment parameter $q < 0$, global warming led to an increase in the values of generalized Hurst indices in the southeast and southwest edges of Bangladesh and a reduction in the values in the northeast regions of Bangladesh (Figure 6c), meaning that due to global warming, the long-range correlation in small fluctuations embedded in daily minimum temperatures was increased in the southeast and southwest edges of Bangladesh and reduced in the northeast regions of Bangladesh (Figure 6c). Similarly, in the case of $q > 0$, global warming led to an increase in the long-range correlation in large fluctuations embedded in daily minimum temperatures in coastal Bangladesh and a reduction in northern Bangladesh (Figure 6f).

4.2. Daily Maximum Temperatures

We calculated generalized Hurst indices $h(q)$ of daily minimum temperatures at all meteorological stations in Bangladesh. Figure 7 demonstrates generalized Hurst indices $h(q)$ at eight stations. It is clear that daily maximum temperatures in Bangladesh exhibited multifractal features, especially as generalized Hurst indices $h(q)$ decay quickly for $q < 0$ and slowly for $q > 0$.

We applied multifractal DFA to the deseasonalized daily maximum temperature data from 1989–2019 and then obtained the distribution of generalized Hurst indices $h(q)$ for different negative and positive values of q in the whole of Bangladesh (Figure 8). Similar to the daily minimum temperature, the generalized Hurst indices of daily maximum temperatures in the whole of Bangladesh were also larger than 0.7 (Figure 8). Such strong persistence implies that historical climatic oscillation modes in each meteorological station have a larger probability of reappearing in the future, resulting in the future evolution of extremely high temperatures at each meteorological station being determined largely by local historical climate change, i.e., the dynamics of extremely high temperature is driven mainly by internal factors. Since the distribution patterns of $h(q)$ for different negative and positive values of q were almost the same (Figure 8), the scaling behavior of small and large fluctuations embedded in daily maximum temperatures shared almost the same spatial pattern. The difference in generalized Hurst indices associated with small and large fluctuations was about 0.16, reflecting that long-range positive correlations of small fluctuations in daily maximum temperatures were higher than that of large fluctuations.

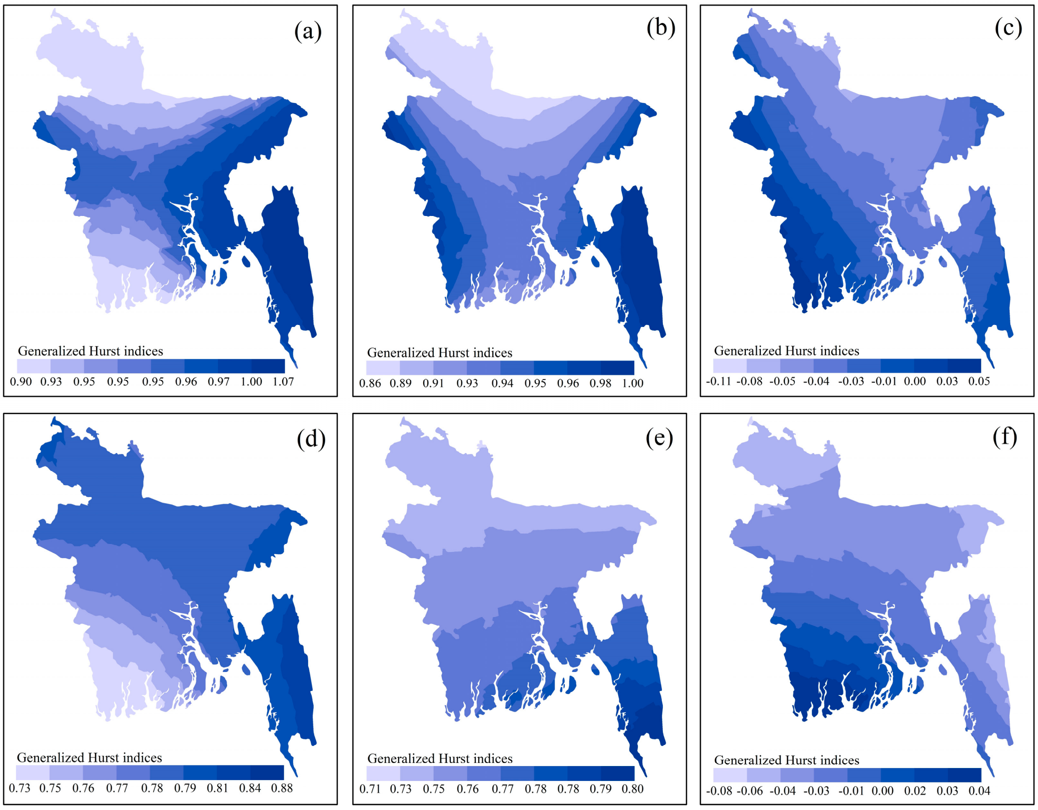

Figure 6. Impacts of global warming on the long-range correlation of daily minimum temperature. The first row demonstrates mean generalized Hurst indices for $q \in [-3, -1]$ during (**a**) [1989–2004], (**b**) [2005–2019], and (**c**) their difference. The second row demonstrates mean indices for $q \in [1, 3]$ during (**d**) [1989–2004] and (**e**) [2005–2019] and (**f**) their differences.

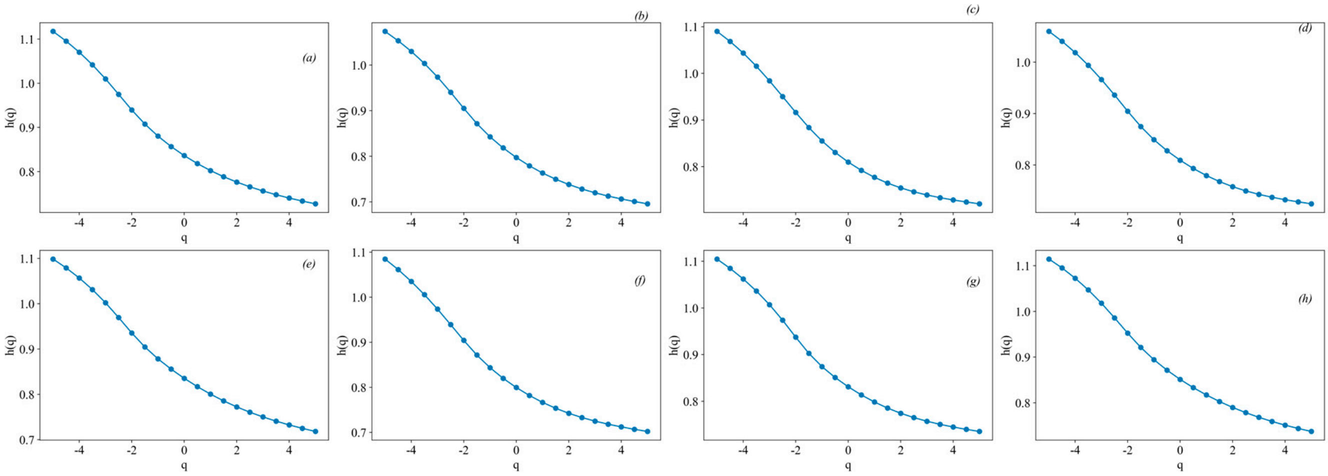

Figure 7. Generalized Hurst indices $h(q)$ of daily maximum temperature at eight meteorological stations: (**a**) Dinajpur, (**b**) Barisal, (**c**) Cox's Bazar, (**d**) Bhola, (**e**) Bogra, (**f**) Chandpur, (**g**) Chittagong, and (**h**) Chuadanga.

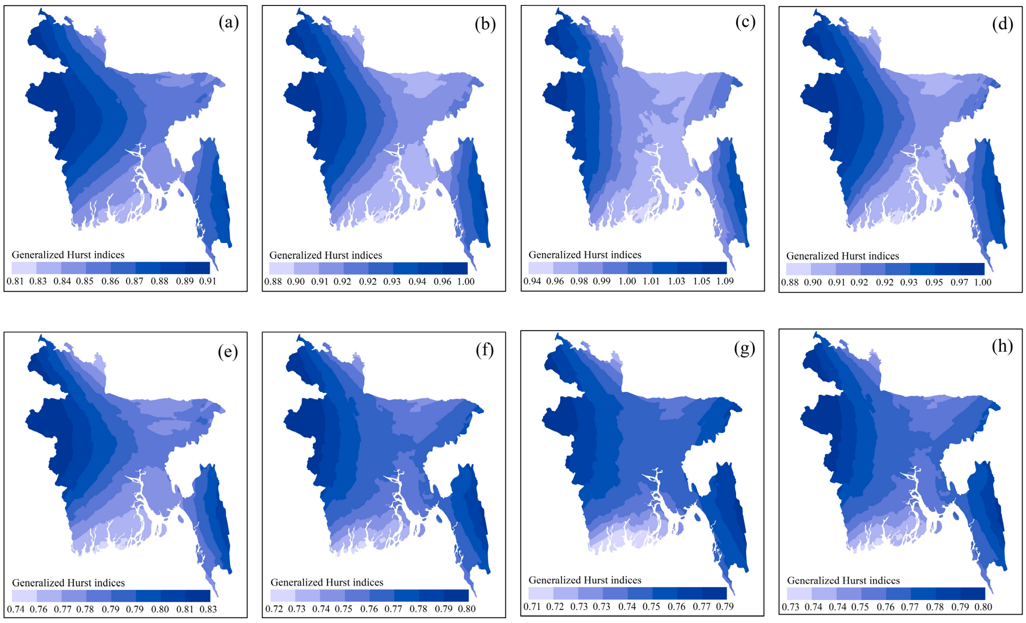

Figure 8. Distribution of (mean) generalized Hurst indices of daily maximum temperatures for (**a**) $q = -1$, (**b**) $q = -2$, (**c**) $q = -3$, (**d**) $q \in [-3, -1]$, (**e**) $q = 1$, (**f**) $q = 2$, (**g**) $q = 3$, and (**h**) $q \in [1, 3]$.

Figure 9 shows the relations between different topographic factors and generalized Hurst indices in Bangladesh. Clearly, these relations were not as strong as those of daily minimum temperatures in terms of R^2. Longitude, latitude, and distance from the coast had impacts on generalized Hurst indices in Bangladesh, but uncertain variability was large (Figure 9). Very roughly, longitude was negatively correlated with generalized Hurst indices in Bangladesh, and latitude and distance from the coast were positively linearly correlated. Noticing that the scaling behavior of both small and large fluctuations in the daily maximum temperature was associated with generalized Hurst indices with moment parameters $q < 0$ and $q > 0$, respectively, it is clear that due to relatively low R^2, longitude, latitude, and distance from the coast had smaller impacts on the scaling behavior of small fluctuations than that of large fluctuations during 1989–2019, but these impacts still passed a statistical significance test (see p-value in Figure 9)

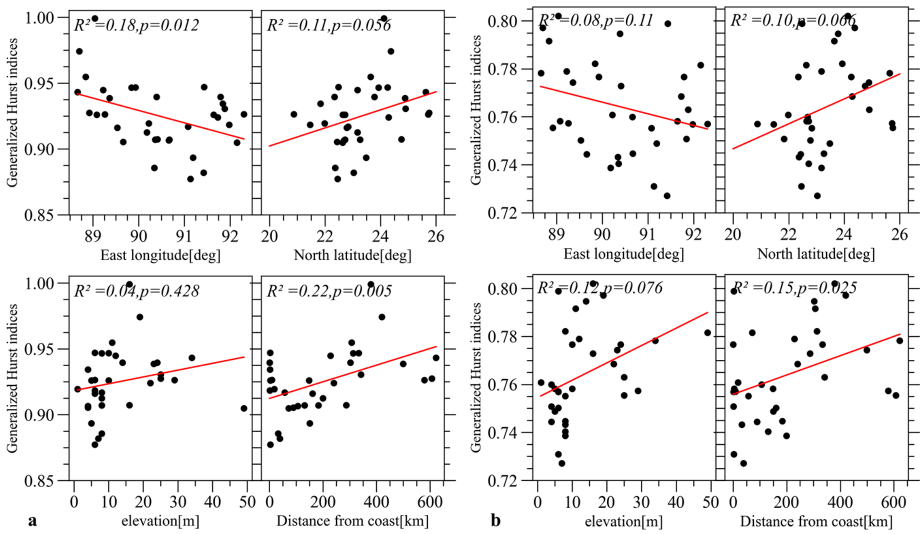

Figure 9. Scatter plots for different topographic factors and mean generalized Hurst indices of daily maximum temperature with (**a**) $q < 0$ and (**b**) $q > 0$.

We investigated the impacts of global warming on the long-range correlation of daily maximum temperatures in Bangladesh (Figure 10). In order to achieve this aim, we divided the whole period [1989–2019] into two periods: [1989–2004] and [2005–2019]. The difference of generalized Hurst indices during the two time periods passed a statistical significance test, and the related significance levels (p values) were 0.019067 ($q = -3$), 0.022923 ($q = -2$), 0.000869 ($q = -1$), 0.001149 ($q = 1$), 3.7931×10^{-6} ($q = 2$), and 0.003397 ($q = 3$). Under global warming impacts, the long-range correlation embedded in daily maximum temperatures was reduced over the whole of Bangladesh (Figure 10c,f). Moreover, the long-range correlation in large fluctuations embedded in daily maximum temperatures was reduced more than that of small fluctuations (Figure 10c,f).

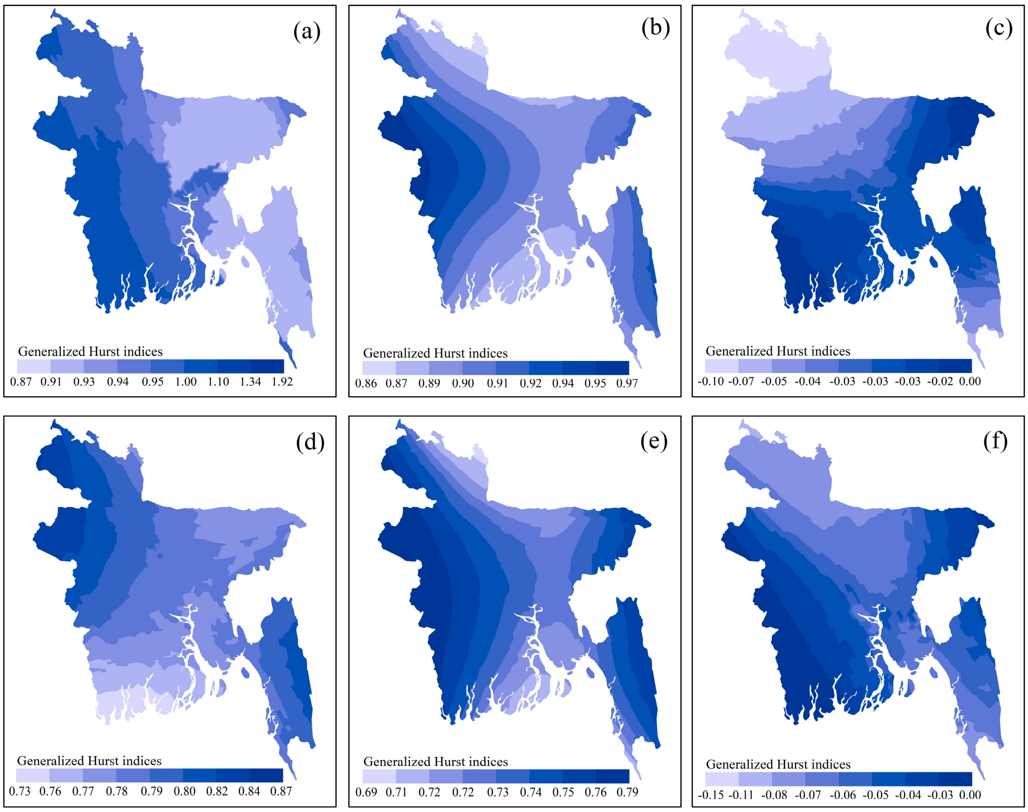

Figure 10. Impact of global warming on the long-range correlation of daily maximum temperatures. The first row demonstrates mean generalized Hurst indices for $q \in [-3, -1]$ during (**a**) [1989–2004], (**b**) [2005–2019], and (**c**) their difference. The second row demonstrates mean indices for $q \in [1, 3]$ during (**d**) [1989–2004] and (**e**) [2005–2019] and (**f**) their differences.

5. Dynamical Thresholds for Temperature Extremes

Extreme temperature events are events in which the number or statistical value significantly deviates from its average temperature state over a specific period [19]. The widely-used ETCCDI climate extreme indices [20] utilize fixed percentile thresholds to roughly determine extreme temperature events. Although various statistical models (e.g., Gumbel distribution and generalized extreme value distribution) may model occurrence frequency and return periods of extreme temperature events, these models still need to use fixed percentile thresholds to discriminate extreme and non-extreme events [21]. Extreme temperature events are only the outlier components in a climate system [21], so their existence cannot significantly affect essential dynamical characteristics of the climate system itself. Due to the difference in dynamical climate evolution among meteorological stations, consistent percentile removal of extreme values may lead to small changes in dynamic mechanisms at some stations and large changes at others. Therefore, it is not a good approach to apply consistent percentile thresholds (e.g., 5%) to discriminate extreme and non-extreme events at all meteorological stations.

Noticing that extreme temperature events always deviate from the mainstream evolution of climate systems, their impacts on the long-range correlation of the whole climate system can be very limited. By utilizing multifractal DFA, we have proposed a dynamical threshold algorithm to divide a temperature time series into extreme and non-extreme events according to their inherent characteristics rather than artificially distinguishing them. The main idea of our dynamic threshold algorithm lies in the fact that the fluctuation functions in multifractal DFA measure the long-range correlation of system evolution over a certain period, so it is hardly affected by extreme values. When extreme values from temperature time series are removed gradually, if the correlation coefficients between the newly generated and original fluctuation functions are almost equal to one (e.g., >99.8%), the removed extreme values just represent temperature extreme events. In detail:

Given a temperature time series $S = \{x_i, I = 1,2, \ldots ,n\}$ with measurement accuracy d, in most cases, d is taken as 0.1 °C.

Step 1. *Denote the maximal value and the minimal value in S by x_{max} and x_{min}, respectively. Initialize two thresholds*

$$T_{max} = x_{max} - d \textit{ and } T_{min} = x_{min} + d.$$

Step 2. *The data larger than T_{max} are removed from the time series S and the remaining time series become*

$$S_{max} = \{x_i,\ x_i < T_{max} \textit{ and } x_i \in S\}$$

and we removed data less than T_{min} from the time series S and the remaining time series is

$$S_{\min} = \{x_i,\ x_i > T_{\min} \textit{ and } x_i \in S\}.$$

Step 3. *For the time series S_{max}, S_{min}, and S, the multifractal DFA is used to obtain three fluctuation functions: $F_q^{max}(s)$, $F_q^{min}(s)$ and $F_q(s)$. Since temperature extremes lead to large fluctuations in time series, only a positive value of q is a token here.*

Step 4. *Calculate the correlation coefficient between $F_q^{max}(s)$ (or $F_q^{min}(s)$) and $F_q(s)$. If the correlation is greater than $1-\epsilon$, then replace T_{max} and T_{min} by $T_{max} - d$ and $T_{min} + d$, respectively, and go to Step 2. Otherwise, terminate the iteration and output two thresholds T_{max} and T_{min}.*

Different from the widely-used ETCCDI climate extreme indices, which use 1%, 5%, or 10% as thresholds, our dynamical threshold algorithm has the key parameter ϵ, which measures the correlation between fluctuation functions of the original time series and the residual after removing extreme values. The key parameter ϵ is suggested to take a small value (e.g., 0.001, 0.002, or 0.003); otherwise, the removal of extreme values from the temperature time series will lead to essential changes in inherent characteristics. In order to guarantee that identified extreme events have the same level of slight impacts on climate fluctuations at all meteorological stations, the same key parameter ϵ must be used to discriminate extreme and non-extreme events at each station, resulting in the percentile thresholds at each station in our algorithm being very different. Therefore, our algorithm dynamically determines thresholds of temperature extremes.

5.1. Extreme Low-Temperature Events in Bangladesh

Applying our dynamic threshold algorithm with $\epsilon = 0.002$ to 1989–2019 daily minimum temperatures observed at 34 meteorological stations of Bangladesh, we determined the thresholds of extreme low-temperature events (Figure 11a). Numerical thresholds for extremely low temperatures had obvious regional differences and ranged from ~8.8 °C in western Bangladesh to ~15 °C in coastal Bangladesh. Northwestern Bangladesh had the lowest thresholds due to the influence of winter monsoons, sea-land distribution, and atmospheric circulation in South Asia. Coastal Bangladesh had the highest numerical thresholds due to the low latitude, a warming ocean, and huge ocean heat capacity. Percentile thresholds were different for each meteorological station and ranged from 5% to 5.64% (Figure 11b).

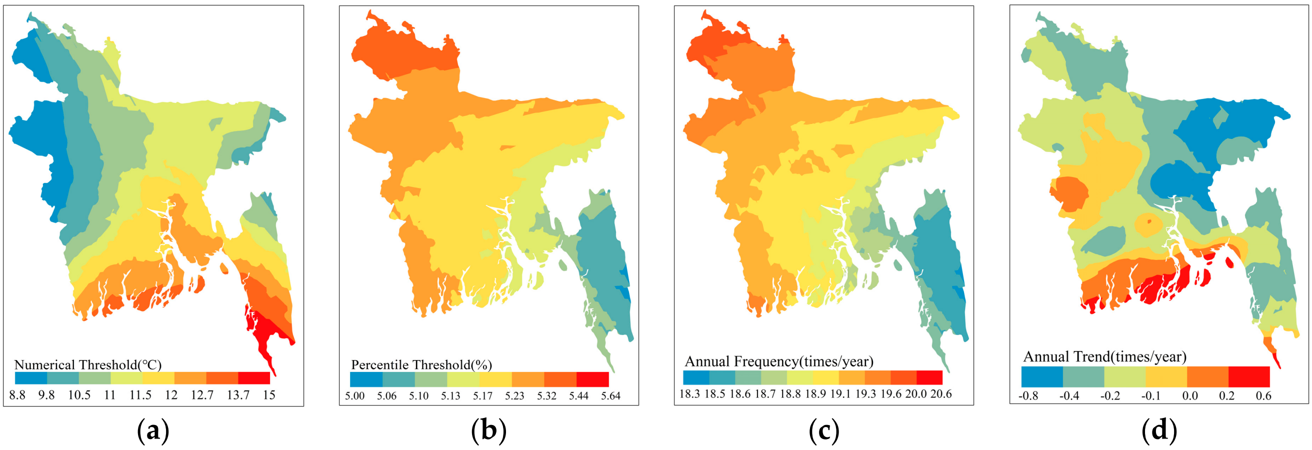

Figure 11. (**a**) Numerical thresholds; (**b**) percentile thresholds; (**c**) mean occurrence frequency; and (**d**) annual trend of extreme low-temperature events in Bangladesh during 1989–2019.

During 1989–2019, the occurrence frequency of extreme low-temperature events gradually decreased from northwest to southeast (Figure 11c). The regional difference was small: northwestern Bangladesh had the highest frequency (20 extreme events per year), while southeastern Bangladesh had the lowest frequency (18 extreme events per year). Since the tropical sea temperature from the lower latitudes had a more significant influence on coastal Bangladesh, a large number of extreme cold events occurred only when winter winds were unusually strong, so the frequency of extreme cold events in coastal Bangladesh was relatively small. Annual trends of extreme low-temperature events in most parts of Bangladesh showed a downward trend (Figure 11d), which is consistent with global warming. But in coastal Bangladesh, the annual trend of extreme low-temperature events had an upward trend.

5.2. Extreme High-Temperature Events in Bangladesh

Applying our dynamic threshold algorithm with $\epsilon = 0.002$ to 1989–2019 daily maximum temperatures observed at 34 meteorological stations of Bangladesh, we determined the threshold for extreme high-temperature events in Bangladesh (Figure 12a). The thresholds for extremely high temperatures in Bangladesh had small regional differences. In most regions of Bangladesh, thresholds were above 34 °C and gradually decreased from west to east, showing a meridional distribution. Western Bangladesh had the highest threshold for extreme high-temperature events. The seasonal movement of the barometric zone and the southwest monsoons of the Indian Ocean led to high temperatures in summer and then a high threshold of extremely high temperatures. Coastal Bangladesh is influenced by huge ocean heat capacity, so the summer temperature in this region was slightly lower, leading to the low threshold of extremely high temperature. Percentile thresholds were different for each meteorological station and ranged from 5% to 9.92% (Figure 12b).

Frequency distribution patterns of extreme high-temperature events in Bangladesh were almost consistent with that of extreme high-temperature thresholds (Figure 12c). Western Bangladesh had the highest frequency (up to 36 extreme events per year), while coastal Bangladesh had the lowest frequency (~18 extreme events per year), demonstrating that high-temperature events occurred more frequently than low-temperature events during 1989–2019. Western Bangladesh is affected by the South Asian summer southwest monsoons and the Indian Depression, so the frequency of extremely high temperatures in western Bangladesh was relatively high. The climate in coastal Bangladesh is affected by huge ocean heat capacity, resulting in the frequency of extreme high-temperature events being relatively low. Between 1989 and 2019, there was an increase in annual extreme high-temperature events in most areas of Bangladesh (Figure 12d). The largest upward trend occurred in coastal Bangladesh. Only near the northwest and southeast borders of Bangladesh did annual extreme high-temperature events show a downward trend.

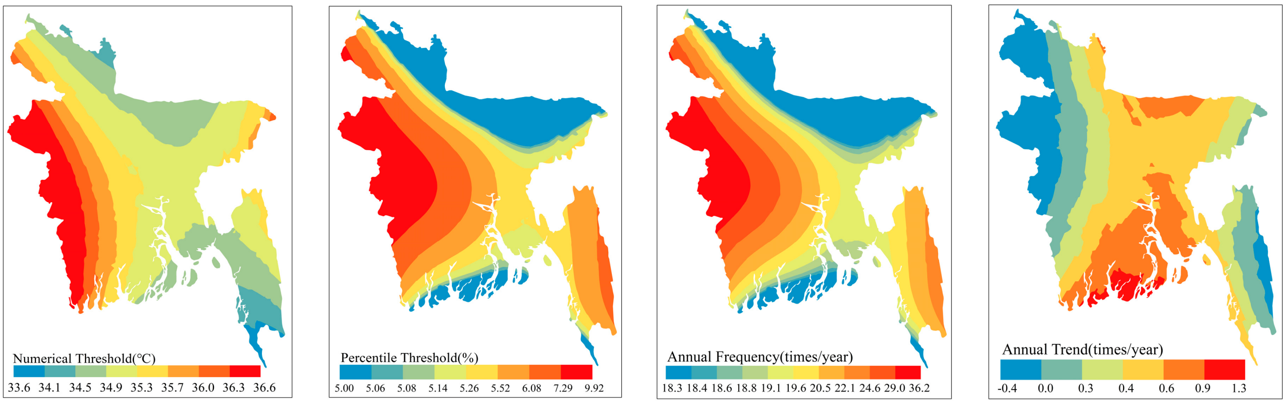

(**a**) (**b**) (**c**) (**d**)

Figure 12. (**a**) Numerical thresholds; (**b**) percentile thresholds; (**c**) mean occurrence frequency; and (**d**) annual trend of extreme high-temperature events in Bangladesh during 1989–2019.

6. Conclusions

Multifractal DFA can extract multi-scaling behavior in climatic time series and then characterize long-range correlations embedded in small and large fluctuations of time series. In this study, with the help of multifractal DFA, we investigated the scaling behavior of daily minimum/maximum temperature data during 1989–2019 from 34 meteorological stations in Bangladesh. We found the following:

➢ The scaling behavior of the daily minimum temperatures in Bangladesh during 1989–2019 demonstrated two different spatial patterns, which corresponded to small and large fluctuations in daily minimum temperatures, respectively. Longitude, latitude, and distance from the coast had significant impacts on scaling behavior with relatively high R^2 values. Moreover, their impacts on the scaling behavior of small fluctuations were larger than that of large fluctuations. Under global warming impacts, the long-range correlation embedded in daily minimum temperatures increased in coastal Bangladesh and increased in northern Bangladesh.

➢ The scaling behavior of the daily maximum temperatures in Bangladesh during 1989–2019 demonstrated only one single spatial pattern. Longitude, latitude, and distance from the coast had some impacts on scaling behavior, but R^2 values were low. Under global warming impacts, the long-range correlation in both small and large fluctuations embedded in daily maximum temperatures was reduced in the whole of Bangladesh.

Extreme temperature events are only the outlier components in a climate system, so their existence cannot significantly affect essential dynamical characteristics of the climate system itself. Due to the difference in dynamical climate evolution among meteorological stations, traditional consistent percentile removal of extreme values may lead to small changes in dynamic mechanisms at some stations and large changes at others. Compared with widely-used percentile thresholds, extreme climate events captured by our algorithm are more reliable since identified extreme events are determined directly by the climate system, and they have the same level of slight impacts on observed climate fluctuations at all meteorological stations. Applying our algorithm to analyze the evolution of extreme climate events in Bangladesh revealed that trends of extreme low-temperature events showed a downward trend, but there was an upward trend in coastal Bangladesh; trends of extreme high-temperature events showed an upward trend, with the largest trends occurring in coastal Bangladesh.

Although this study focuses only on Bangladesh, analysis and our proposed algorithm can be easily extended to reveal spatial patterns, topographic impacts, and global warming impacts of the scaling behavior (or long-range correlations) of climate evolution and related extreme events in other countries and regions.

Author Contributions: Conceptualization, Z.Z.; Methodology, Z.Z.; Software, A.L.; Formal analysis, Z.Z. and M.J.C.C.; Data curation, A.L. and L.C.D.; Writing—original draft, Z.Z.; Writing—review & editing, Z.Z. and M.J.C.C.; Visualization, A.L.; Project administration, Z.Z.; Funding acquisition, Z.Z. All authors have read and agreed to the published version of the manuscript.

Funding: The corresponding author was supported by the European Commission Horizon 2020 Framework Program No. 861584 and the Taishan Distinguished Professor Fund No. 20190910.

Data Availability Statement: Not applicable.

Conflicts of Interest: The authors declare no conflict of interest.

References

1. Intergovernmental Panel on Climate Change (IPCC). *Climate Change 2023: The Physical Science Basis*; Intergovernmental Panel on Climate Change (IPCC): Geneva, Switzerland, 2023.
2. Shukla, J. Predictability in the Midst of Chaos: A scientific basis for climate forecasting. *Science* **1998**, *282*, 728–731. [CrossRef] [PubMed]
3. Peng, C.K.; Buldyrev, S.V.; Havlin, S.; Simons, M.; Stanley, H.E.; Goldberger, A.L. Mosaic organization of DNA nucleotides. *Phys. Rev. E* **1994**, *49*, 685–1689. [CrossRef] [PubMed]
4. Tatli, H.; Dalfes, H.N. Long-time memory in drought via detrended fluctuation analysis. *Water Resour. Manag.* **2020**, *34*, 1199–1212. [CrossRef]
5. Kurnaz, M.L. Detrended fluctuation analysis as a statistical tool to monitor the climate. *J. Stat. Mech. Theory Exp.* **2004**, *2004*, P07009. [CrossRef]
6. Orun, M.; Koçak, K. Applicatıon of detrended fluctuation analysis to temperature data from Turkey. *Int. J. Climatol. A J. R. Meteorol. Soc.* **2009**, *29*, 2130–2136. [CrossRef]
7. Telesca, L.; Pierini, J.O.; Scian, B. Investigating the temporal variation of the scaling behavior in rainfall data measured in central Argentina by means of detrended fluctuation analysis. *Phys. A Stat. Mech. Its Appl.* **2012**, *391*, 1553–1562. [CrossRef]
8. Kalamaras, N.; Philippopoulos, K.; Deligiorgi, D.; Tzanis, C.G.; Karvounis, G. Multifractal scaling properties of daily air temperature time series. *Chaos Solitons Fractals* **2017**, *98*, 38–43. [CrossRef]
9. Gómez-Gómez, J.; Carmona-Cabezas, R.; Ariza-Villaverde, A.B.; de Ravé, E.G.; Jiménez-Hornero, F.J. Multifractal detrended fluctuation analysis of temperature in Spain (1960–2019). *Phys. A Stat. Mech. Its Appl.* **2021**, *578*, 126118. [CrossRef]
10. Avotniece, Z.; Rodinov, V.; Lizuma, L.; Briede, A.; Klavins, M. Trends in the frequency of extreme climate events in Latvia. *Baltica* **2010**, *23*, 135–148.
11. Easterling, D.R.; Meehl, G.A.; Parmesan, C.; Changnon, S.A.; Karl, T.R.; Mearns, L.O. Climate extremes: Observations, modeling, and impacts. *Science* **2000**, *289*, 2068–2074. [CrossRef] [PubMed]
12. Hoque, M.A.A.; Pradhan, B.; Ahmed, N. Assessing drought vulnerability using geospatial techniques in northwestern part of Bangladesh. *Sci. Total Environ.* **2020**, *705*, 135957. [CrossRef] [PubMed]
13. Rahman, M.R.; Lateh, H. Climate change in Bangladesh: A spatio-temporal analysis and simulation of recent temperature and rainfall data using GIS and time series analysis model. *Theor. Appl. Climatol.* **2017**, *128*, 27–41. [CrossRef]
14. Banerjee, O.; Mahzab, M.; Raihan, S.; Islam, N. An economy-wide analysis of climate change impacts on agriculture and food security in Bangladesh. *Clim. Chang. Econ.* **2015**, *6*, 1550003. [CrossRef]
15. Agrawala, S.T.O.; Ahmed, A.U.; Smith, J.; Aalst, M.V. *Development and Climate Change in Bangladesh: Focus on Coastal Flooding and the Sunder Bans*; Organization for Economic Co-Operation and Development (OECD): Paris, France, 2003.
16. Peng, C.-K.; Havlin, S.; Stanley, H.E.; Goldberger, A.L. Quantification of scaling exponents and crossover phenomena in nonstationary heartbeat time series. *Chaos* **1995**, *5*, 82. [CrossRef] [PubMed]
17. Kantelhardta, J.W.; Zschiegner, S.A.; Bunde, E.K.; Havlin, S.; Bunde, A.; Stanley, H.E. Multifractal detrended fluctuation analysis of nonstationary time series. *Phys. A* **2002**, *316*, 87–114. [CrossRef]
18. Zheng, Z. Characteristics of long-term climate change in Beijing with Detrended Fluctuation Analysis. In Proceedings of the 2010 Sixth International Conference on Natural Computation, Yantai, China, 10–12 August 2010; IEEE: Piscataway, NJ, USA, 2010; Volume 2, pp. 1084–1088.

19. Zhang, X.; Hegerl, G.; Zwiers, F.W.; Kenyon, J. Avoiding inhomogeneity in percentile-based indices of temperature extremes. *J. Clim.* **2005**, *18*, 1641–1651. [CrossRef]
20. Zhang, X.; Alexander, L.; Hegerl, G.; Jones, P.; Klein, T.A.; Peterson, T.C.; Trewin, B.; Zwiers, F.W. Indices for monitoring changes in extremes based on daily temperature and precipitation data. *Wiley Interdiscip. Rev. Clim. Chang.* **2011**, *2*, 851–870. [CrossRef]
21. Mudelsee, M. *Climate Time Series Analysis*; Springer: Cham, Switzerland, 2014.